

Metal–Insulator Transition of Ge–Sb–Te Superlattice: An Electron Counting Model Study

Nian-Ke Chen, Xian-Bin Li^{1b}, *Member, IEEE*, Xue-Peng Wang, Sheng-Yi Xie, Wei Quan Tian, Shengbai Zhang, and Hong-Bo Sun^{2b}, *Fellow, IEEE*

Abstract—Ge–Sb–Te superlattice (GST-SL) is a newly emerging electronic material for nonvolatile phase-change memory with ultralow energy cost. However, its switching mechanism is still unclear with intensive debates. In this work, by first-principles calculations and an electron counting model study, we study the possible mechanism of phase change and the accompanying property transition of GST-SL. GST-SL are separated into individual layers by van der Waals gaps. We demonstrate that both the global chemical stoichiometry of the material and the local chemical stoichiometry of individual layer block are required to have an insulating band gap according to an electron counting model analysis. The electrical property can be adjusted by changing the local stoichiometry, such as producing defects around van der Waals gaps. Inspired by a previous experiment, we propose that a stacking-fault motion can spontaneously alter the band gap and results in a metal–insulator transition. This transition may provide a significant change of carrier concentration and indicate an ultralow energy-consumption process with a low energy barrier. The present investigations reveal a picture of electrical transition in GST-SL and may guide us to improve its device performances.

Index Terms—First-principles calculations, metal–insulator transition, phase change memory.

Manuscript received November 14, 2017; accepted November 25, 2017. Date of publication December 6, 2017; date of current version January 8, 2018. This work, at JLU, was supported by the National Key Research and Development Program of China and National Natural Science Foundation of China under Grants 2017YFB1104300, 61590930, 2014CB921303, 11374119, and 61775077. The work of S. Zhang was supported by the Department of Energy under Grant DE-SC0002623. The work of W. Q. Tian was supported in part by the Open Project of Key Laboratory of Polyoxometalate Science of Ministry of Education (NENU) and in part by the State Key Laboratory of Supramolecular Structure and Materials (JLU) under Grant SKLSSM201723. The review of this paper was arranged by Associate Editor Y. H. Cho. (*Corresponding author: Xian-Bin Li.*)

N.-K. Chen, X.-B. Li, and X.-P. Wang are with the State Key Laboratory of Integrated Optoelectronics, College of Electronic Science and Engineering, Jilin University, Changchun 130012, China (e-mail: lixianbin@jlu.edu.cn).

S.-Y. Xie is with the School of Physics and Electronics, Hunan University, Changsha 410082, China.

W. Q. Tian is with the College of Chemistry and Chemical Engineering, Chongqing University, Chongqing 401331, China.

S. Zhang is also with the Department of Physics, Applied Physics, and Astronomy, Rensselaer Polytechnic Institute, Troy, NY 12180 USA, and also with the State Key Laboratory of Integrated Optoelectronics, College of Electronic Science and Engineering, Jilin University, Changchun 130012, China.

H.-B. Sun is also with the Department of Precision Instrument, Tsinghua University, Beijing 100084, China, and also with the State Key Laboratory of Integrated Optoelectronics, College of Electronic Science and Engineering, Jilin University, Changchun 130012, China.

Color versions of one or more of the figures in this paper are available online at <http://ieeexplore.ieee.org>.

Digital Object Identifier 10.1109/TNANO.2017.2779579

I. INTRODUCTION

PHASE change memory (PCM) is a promising technology for non-volatile information storage with fast speed and high density which are urgently needed in the big data era [1]–[5]. Meanwhile, PCM is also an important candidate for some other advanced applications such as flexible display [6], thermal emitter [7], and artificial intelligence [8]. Some performances of present PCM devices, such as the speed and the signal contrast, are good enough for random access memory, however, the power consumption should be further lowered to achieve high-density integrations. For example, although Ge₂Sb₂Te₅ alloy is the flagship PCM material [9]–[11], the RESET power consumption based on Ge₂Sb₂Te₅ is still too high [4], [12], [13]. Recently, a new type of PCM material named Ge–Sb–Te superlattice (GST-SL) has drawn many attentions due to its ultralow power consumption [14]. This excellent performance has been attributed to a unique data-storage mechanism: crystalline-to-crystalline phase change [14]–[16]. Compared with the conventional crystalline-to-amorphous phase change [17]–[20], this mechanism has a smaller conformational-entropy difference between the two phases, and thus reduces the energy consumption for switching.

Several mechanisms of the GST-SL switching have been proposed in previous reports. Takaura *et al.* suggested a carrier injection induced flipping of two GeTe bilayers, which results in a transition between the Petrov and the Inverted-Petrov structures [21]. Tominaga *et al.* suggested an electrical field induced flipping of Ge layers, which results in a transition between the Ferro and the Inverted-Petrov structures (flip-flop mechanism) [15]. Yu *et al.* studied the phase-transition paths and the energy barriers between the Ferro/Petrov and the Inverted Petrov structures [22], where they proposed a 2-step phase change mechanism with an energy barrier larger than 2.56 eV. The works of Kalikka *et al.* [23] and Zhou *et al.* [24] suggested that the strain in GST-SL makes the partial melting of GeTe layer become possible. Ohyanagi and Takaura revealed that the active region of the GST-SL is adjacent to the electrodes [25]. Momand *et al.* argued that the most stable phase of the GST-SL is similar to the Kooi model with the rhombohedral GeSbTe layers [26]. Despite so many explanations, a widely accepted model is still missing, which hinders the further development or optimization of the GST-SL devices.

In fact, to achieve a PCM device with a low energy consumption, a critical way is to achieve enormous change of the electrical property but with slight variation of the structure, and the

difficulty is to realize the phase transition with a low energy barrier. For example, the energy barrier for the flip-flop mechanism is larger than 2.56 eV which is too high for an ultrafast (\sim ns) phase transition [22]. As such, a mechanism of the phase transition accompanying with a large electrical-property transition as well as a low energy barrier in GST-SL is urgently needed.

In the present work, we propose a switching mechanism based on electron counting model (ECM) analysis [27], [28], *i.e.*, a mechanism about metal-insulator transition (MIT) in GST-SL. This transition is achieved by stacking-fault motions without amorphization. We demonstrate that in GST-SL the stacking-fault movement turns the material into a metallic state due to breaking the local chemical stoichiometry. As such, the transition can provide a significant electrical-property contrast for memory. Meanwhile, this transition is an order-to-order phase change which reduces energy consumption for switching. Compared with previous reports, the phase transition barrier of this mechanism can be as low as 0.6 eV. The present work reveals a feasible mechanism of electrical switching in GST-SL which may help to improve devices with low energy consumption.

II. METHOD

Calculations are carried out based on density functional theory (DFT) as implemented in VASP code [29], [30]. The projector augmented wave (PAW) pseudopotential [31] and the Perdew–Burke–Ernzerhof (PBE) exchange–correlation functional [32] are used in the calculations. In GeTe/Sb₂Te₃ superlattice, the interaction between layered GeTe and Sb₂Te₃ is a weak van der Waals (vdW) interaction which is described by the London dispersion interaction [33]. While popular density functionals are successful in the description of strong chemical bonds (such as the covalent, the ionic and the metallic bonds), they are insufficient to describe correctly vdW interactions. So, corrections of the DFT-D2 method of Grimme scheme [34] is used to add a semi-empirical dispersion potential to the conventional Kohn-Sham DFT energy [35]: $E = E_{DFT-KS} + E_{dispersion}$. Parameters used in this work follow those of Grimme [34]. The structural models can be divided into three categories with different sizes (144, 192 and 384 atoms, respectively) to illustrate different issues (The reason is explained in the following section). All models have been fully relaxed until the total energy and atomic forces are converged to less than 1×10^{-5} eV and 0.01 eV/Å, respectively. The energy cutoff for plane-wave expansion is 240 eV. The K-point grids for the models with 144 and 192 atoms are $2 \times 2 \times 2$ while the K-point grids for the models with 384 atoms are $1 \times 2 \times 2$. The electronic spin is considered in our calculations. But there are no net magnetic moments in all of our models. The energy barrier is calculated using the Nudged Elastic Band (NEB) method [36]–[38]. The structural models are shown with VESTA software package [39].

III. RESULTS AND DISCUSSIONS

GST-SL possesses layered structures. Until now, there are four popular models with different layer sequences for the superlattice (Here, we take the composition of Ge₂Sb₂Te₅ as an example. They are named Ferro, Petrov, Inverted-Petrov and

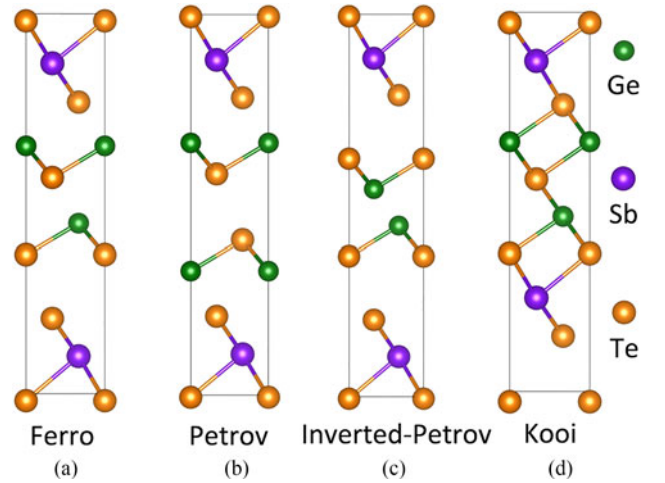


Fig. 1. The four popular models of GST-SL. The green, purple and orange balls are Ge, Sb and Te atoms, respectively.

Kooi models [Fig. 1(a)–(d)]. According to previous reports [15], [26], [40], the Kooi model is most stable at low temperatures and also has been observed in experiments by TEM. The atomic coordination and chemical bonds in the Kooi model are easy to be identified. As such, it is convenient to carry out the electron counting analysis in the Kooi model. In fact, the electron counting model has been successful to explain the link between the structure and properties, such as surface reconstruction problem for semiconductors [28]. According to this analysis, the net charge transfer within a formula unit of a material should be zero in order to hold a band gap [27]. For example, in the Kooi model (Ge₂Sb₂Te₅), a Ge or Sb atom can be considered to donate two (+2) or three (+3) p electrons while a Te atom accepts two electrons (−2). Here, the electron counting is as follows: $2 \times 2 + 2 \times 3 - 5 \times 2 = 0$. Therefore, a perfect stoichiometric Kooi model [Fig. 2(a) left] can be a semiconductor with a well-defined band gap. This is demonstrated by the density of states (DOS) in Fig. 2(b). If the chemical composition is non-stoichiometric, the electron counting will not be zero. For example, when a part of Sb atoms in the Kooi model are substituted by some Ge atoms [Fig. 2(a) right], the electrons in the system are deficient. Then, the DOS shows that the Fermi-level shifts down into the valence band which indicates becoming metallic [Fig. 2(b)]. Here, we find that a 3% such substitution is enough to change the original semiconductor to a metal.

As discussed above, breaking the global chemical stoichiometry is an easy way to change property. However, the global composition of a material is nearly constant after it has been synthesized. An alternative way proposed here is to break the local stoichiometry by manipulating local defects while the global composition is retained. For instance, it has been reported that Ge and Sb atoms are easily intermixed during the growth of GST-SL [41]. This result has been confirmed by TEM [26], EXAFS [42], and first-principles calculations [40]. According to previous reports, the intermixing has several influences on material properties. First, it influences the stability of GST-SL [40], [42]. In the Kooi model, theoretical calculations have demonstrated that a structure with Ge/Sb intermixing less than

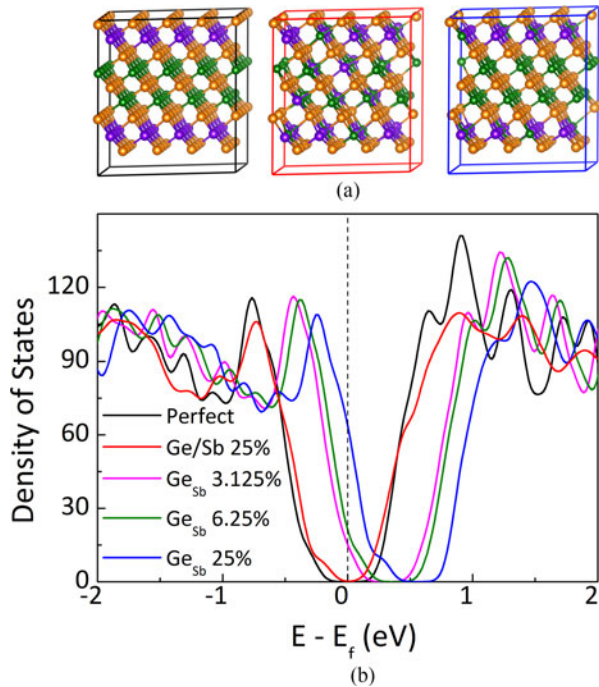


Fig. 2. (a) The structures of perfect (left, the Kooi model), 25% Ge/Sb intermixed (middle, 25% Sb atoms are intermixed with Ge atoms), and 25% Ge_{Sb} substituted (right, 25% Sb atoms are substituted by Ge atoms) GST-SL. (b) Density of states of the perfect, 25% Ge/Sb intermixed (Ge/Sb 25%) and X% Ge_{Sb} substituted (Ge_{Sb} X%, X% Sb atoms are substituted by Ge atoms. X = 3.125, 6.25 and 25) structures. The green, purple and orange balls are Ge, Sb and Te atoms, respectively. Here, models with 144 atoms are used to describe the intermixing in a single layer block.

50% can further lower the total energy. [40]. Second, the intermixing can introduce Peierls distortion in GST-SL that may provide a meta-stable phase [40]. Third, the intermixing leads to a formation of GST-alloy layer which may increase the band gap and thereby decrease the electrical conductance [26], [43].

However, according to our study, the intermixing alone in a single layer block of GST-SL cannot change the electronic DOS significantly. According to a former report, the structure of the Kooi model with 25% Ge/Sb intermixing (i.e., 25% Sb atoms are intermixed with Ge atoms) is most stable among various intermixing situations [40]. Therefore, we calculate the DOS in a GST-SL with such an intermixing ratio in a single layer block [Fig. 2(a) middle]. Fig. 2(b) shows that the band gap just changes slightly (from 0.6 to 0.4 eV) and indeed it is still a semiconductor. In fact, this is also backed by the electron counting model because the net charge transfer in the same block is still zero. In other words, although the intermixing can induce local chemical disorders in GST-SL, it is not enough to change the electronic properties significantly.

Next, in order to change the electrical property, we may have to find another way to control local chemical disorders in GST-SL. It is known that a large amount of vdW gaps split the GST-SL into many layer blocks. Each block is locally stoichiometric. Fig. 3(a) shows a GST-SL model that is composed of two layer blocks per unit. The upper one is a layer block of Ge₁Sb₂Te₃ that is similar to the Kooi model and the lower one

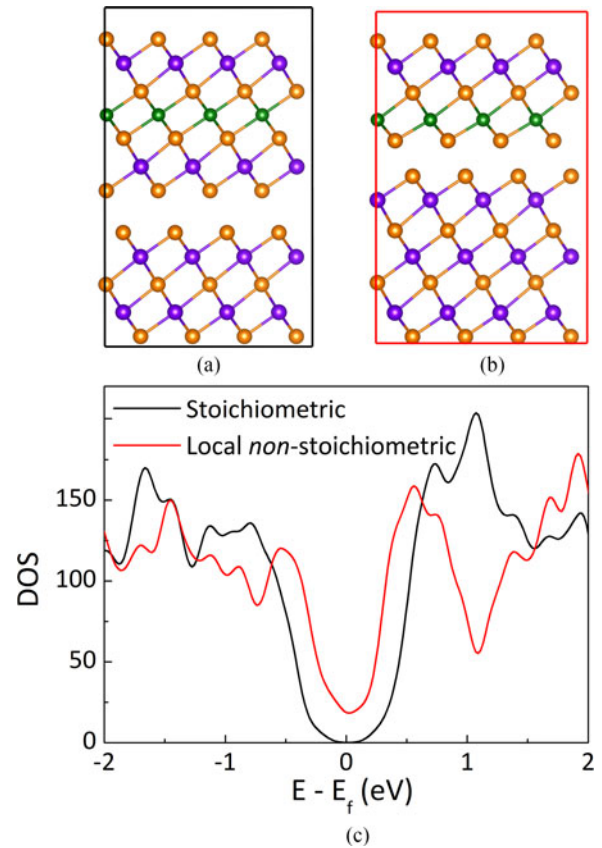


Fig. 3. (a) The stoichiometric and (b) the non-stoichiometric models. (c) DOS of the two models. The green, purple and orange balls are Ge, Sb and Te atoms, respectively. Here, models with 192 atoms are used to describe the local stoichiometry which needs at least two vdW gaps.

is a quintuple layer of Sb₂Te₃. Both of the two blocks have been definitely observed in GST-SL by TEM [26]. According to the electron counting model, both of the blocks are chemically stoichiometric and Fig. 3(c) indeed shows a well-defined band gap of about 0.4 eV. Fig. 3(b) shows another model with the same global composition but the different local composition: the upper block has a composition of GeSbTe₃ while the lower block has a composition of Sb₃Te₄. This new model can be achieved by flipping a Sb layer in the first model. Here, we do the electron counting analysis for the upper block: $1 \times 2 + 1 \times 3 - 3 \times 2 = -1$ (electrons are deficient) and the lower block: $3 \times 3 - 4 \times 2 = 1$ (electrons are surplus). In other words, both of the layer blocks are non-stoichiometric. Indeed, Fig. 3(c) demonstrates that the material turns into a metallic phase without a band gap. In sum, not only the global chemical composition but also the local composition for every layer block should be stoichiometric to hold a band gap. With the vdW gaps between layer blocks, we may adjust electrical properties for GST-SL by changing the local compositions.

Naturally, a key issue is to find a concrete route to change local composition and then control electrical property of GST-SL. In fact, the energy barrier for flipping Sb atomic layer is about 3.3 eV [22] that is large enough to prevent the event even at its melting point. According to the Arrhenius equation, the

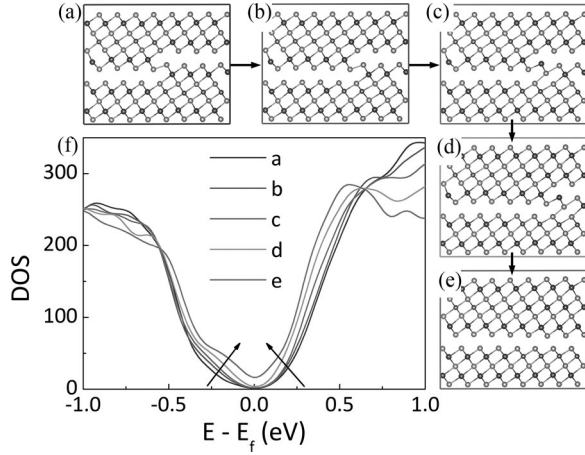


Fig. 4. (a)-(e) The movements of a stacking fault lead to the change of the electrical property. The movements are achieved by Sb atom flipping. (f) The DOS of these structures. The two arrows in f indicate the variation tendency of band gaps along with the movements of stacking faults. The green, purple and orange balls are Ge, Sb and Te atoms, respectively. Here, models with 384 atoms are used to describe the stacking-fault motion, which should be large enough to contain a stacking fault. The sizes of our models are close to the limit of the current DFT calculations. Although these sizes are relatively small comparing to the sizes of the real devices, they should be enough to quantitatively illustrate the electron counting model analysis in the present study, i.e., the change of the local chemical stoichiometry induced by the stacking-fault motion is clearly demonstrated to lead to the electrical property transitions.

flipping rate coefficient k can be expressed as:

$$k = Ae^{-E_a/K_B T}$$

where A is the frequency factor, E_a is the activation energy (per molecule or atom), K_B is the Boltzmann constant and T is the absolute temperature. For the flipping behavior, A is the vibration frequency of the atoms. In GST-SL, the dominant phonon frequency is around 3.48 THz [44]. Here, taking $A = 3.48$ THz (3.48×10^{12} s⁻¹), $E_a = 3.3$ eV (per atom) and $T = 900$ K (close to the melting point), we get an estimated flipping rate coefficient of 1.5×10^{-6} s⁻¹. This rate coefficient means that the time of flipping is about 666667 s, which means it is quite difficult for PCM devices to realize fast data storage. Moreover, if the flipping of Sb layer is a collective behavior, the frequency factor A should be much smaller and the total activation energy E_a should be much larger. As such, the collective flipping of Sb layer is nearly impossible.

However, the flipping of Sb layer could be realized with aids of defects around the vdW gaps. For example, some experiments have reported the existences of stacking faults in GST-SL [26]. Using TEM analysis, the Kooi model has been observed by a 400 °C annealing, where the cation layers adjacent to the vdW gaps are the Sb layers rather than the Ge layers. Fig. 4(a) shows a model of global stoichiometric GST-SL (with a composition of Ge₁Sb₄Te₇) containing a stacking fault. Here, the block with 5 atomic layers is the Sb₂Te₃ quintuple layer while the block with 7 atomic layers is the Kooi model of Ge₁Sb₂Te₄. It is obvious that the local chemical composition is stoichiometric both in the right side and the left side of the stacking fault. The calculated DOS demonstrates that it is a semiconductor with a

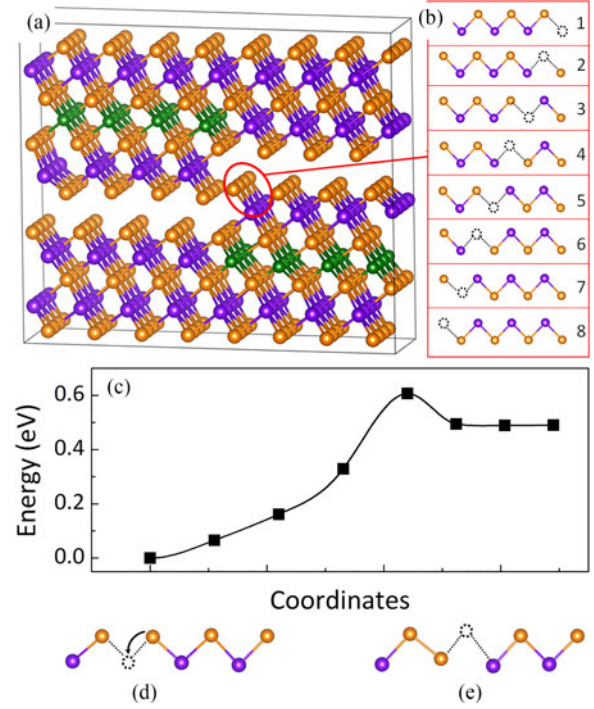


Fig. 5. The schematic for the mechanism of vacancy-assisted stacking fault movement as reported by Yu *et al.* [35]. (a) The structure displays the stacking fault in GST-SL. The two rows of Sb-Te atoms in the red circle locate at the boundary of the stacking fault. (b) A zoom of for the two Sb-Te rows in form of a zigzag chain as displayed in the red square. There is a Sb vacancy (indicated by the dashed circles) in the chain (step 1). The vacancy can move along this chain through the one-by-one movement of Sb and Te atoms (from step 1 to 8). As a result, the positions of Sb and Te atoms are exchanged (step 8), which leads to the motion of the stacking fault. The green, purple and orange spheres are Ge, Sb and Te atoms, respectively.

well-defined band gap [Fig. 4(f)], which is consistent with the electron counting model analysis.

Experimental observations have demonstrated that the stacking faults in GST-SL can move during annealing [45]. In fact, the flipping of Sb layer between the two layer blocks can be realized by the movement of the stacking fault [Fig. 4(b)-(e)]. During this process, the Sb and Te atoms at the boundary of the stacking fault exchange their positions. Yu *et al.*, have investigated the movements of stacking faults in GST-SL [40]. They calculated the energy barriers of three mechanisms. The barriers for the direct atom exchange mechanism, the snake-like collective motion mechanism and the vacancy assisted one-by-one movement mechanism are 3.3 eV, 1.6 eV and 0.5-0.7 eV, respectively. According to the Arrhenius equation, the time of the flipping in the three mechanisms (under 900 K) are 6.7×10^5 s, 2.3×10^{-4} s, and $175 - 2269 \times 10^{-12}$ s, respectively. Fig. 5 illustrates the atomic picture for the last mechanism which is most energy favorable. Fig. 5(a) shows the GST-SL structure with a stacking fault. Fig. 5(b) highlights the Sb-Te atom chains at the boundary of the stacking fault. This mechanism supposes the existence of Sb vacancy [10]. As displayed in Fig. 5(b), with the help of the vacancy, Sb and Te atoms move one-by-one along the chain and finally result in the exchange of positions of Sb and Te atoms, see from step 1

to step 8. We also calculate the energy barrier for the first-step flipping [Fig. 5(c)]. The energy barrier is about 0.61 eV which agrees well with 0.5–0.7 eV in previous report [40].

Here, the mechanism is illustrated in a row of atoms [i.e., the zigzag chain marked by the red circle in Fig. 5(a)], but we do not mean that the flipping only occurs row by row. Actually, after part of the first-row atoms have flipped, the second-row atoms can start to flip. Similarly, the atoms of the third row, the fourth row, the fifth row . . . can take place in turn. In this way, the stacking fault movements can be activated by feasible thermal motions. In this mechanism, the vacancies supply space for atomic motions and thus facilitate the phase transitions. However, for the one-by-one atomic flipping, one flipping event can eliminate a vacancy but simultaneously produces another new vacancy. So, the transition just needs a very small amount of vacancies which should not affect the electronic property much in GST-SL.

Although the global stoichiometry is maintained, after the movement of the stacking fault, the local stoichiometry is broken [Fig. 4(b)–(e)]. For example, after the stacking fault movement, the superlattice is separated into another two layer blocks [Fig. 4(e)], where the local composition of the upper block is $\text{Ge}_{16}\text{Sb}_{80}\text{Te}_{128}$ while the composition of the lower block is $\text{Ge}_{16}\text{Sb}_{48}\text{Te}_{96}$. Then, we do the electron counting model analysis for the upper block: $16 \times 2 + 80 \times 3 - 128 \times 2 = 16$ and for the lower block: $16 \times 2 + 48 \times 3 - 96 \times 2 = -16$. In other words, the electrons in the upper block of the superlattice are surplus while the electrons in the lower block of the superlattice are deficient. From the calculated DOS, the band gaps gradually decrease to zero with the movement of stacking fault [Fig. 4(f)]. Finally, the material turns into a metal.

Fig. 6 further displays the carrier concentration for the models during the stacking-fault motion. The concentration is estimated by the integration of the DOS and Fermi-Dirac distribution function at a certain finite temperature. The number of electrons and holes excited by thermal energy is approximately $N_e = \int_{E_f}^{\infty} \text{DOS} \cdot f_{\text{FD}}(E, T) dE$, and $N_h = \int_{-\infty}^{E_f} \text{DOS} [1 - f_{\text{FD}}(E, T)] dE$, respectively. DOS is the density of states. $f_{\text{FD}}(E, T) = \frac{1}{\exp(\frac{E-E_f}{k_B T}) + 1}$ is the Fermi-Dirac distribution function. E_f is the Fermi level. k_B is the Boltzmann constant and T is the absolute temperature. Using the DOS in Fig. 4(f) and $T = 300$ K at room temperature, the carrier concentrations $n = (N_e + N_h)/V$ (V is the volume) for the models in Fig. 4 are estimated (Fig. 6). As a result, the carrier concentration indeed significantly increases during the transition. Therefore, the movement of the stacking fault results in a MIT in GST-SL.

The energy landscape of flipping [Fig. 5(c)] indicates that the insulating and metallic phases are bistable states at room temperature. The total energy of the metallic phase [Fig. 4(e)] is higher than that of the insulating phase [Fig. 4(a)]. A high-energy (electrical or optical) pulse can drive the transition from low-energy phase to high-energy phase. Then, a mild-energy pulse can turn it back to the original low-energy phase. The detailed mechanism of reversibility and the control of the stacking-faults motions still need further explorations.

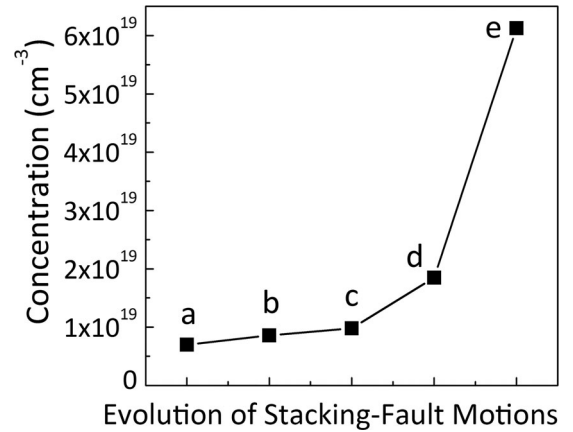


Fig. 6. The change of carrier concentration close to Fermi level during the stacking-fault motion in Fig. 4. The data labelled by a–e correspond to the models of a–e in Fig. 4, respectively. The concentration is obtained by integrating the DOS and Fermi-Dirac distribution function as stated in the main text.

IV. CONCLUSION

In summary, this work has explored a MIT mechanism in GST-SL. By first-principles calculations and electron counting model analysis, we found a way to control the electronic property of GST-SL by motions of stacking faults. We demonstrate that the motion can break the local chemical stoichiometry in GST-SL and leads to MIT. This transition can provide obvious change of carrier concentration. Comparing to the conventional phase change between crystalline states and amorphous states, this order-to-order MIT may reduce the switching energy significantly. Interestingly, the energy barrier for this transition can be as low as 0.6 eV assisted by vacancy. We expect that such transition should also be affected by electrical or laser pulse, which are still not considered here. On the other hand, the reversibility of the present proposed MIT is still not clear and need further exploration. Anyway, the present study offers an updated picture to under the property change in GST-SL which may benefit their device design.

ACKNOWLEDGMENT

The authors would like to thank the HPCC at JLU for providing the supercomputer time.

REFERENCES

- [1] S. Ovshinsky, “Reversible electrical switching phenomena in disordered structures,” *Phys. Rev. Lett.*, vol. 21, no. 20, pp. 1450–1453, 1968.
- [2] M. Wuttig, “Phase-change materials: Towards a universal memory?” *Nature Mater.*, vol. 4, pp. 265–266, 2005.
- [3] M. Wuttig and N. Yamada, “Phase-change materials for rewritable data storage,” *Nature Mater.*, vol. 6, pp. 824–832, 2007.
- [4] M. Zhu *et al.*, “One order of magnitude faster phase change at reduced power in Ti-Sb-Te,” *Nature Commun.*, vol. 5, 2014, Art. no. 4086.
- [5] O. L. Muskens *et al.*, “Antenna-assisted picosecond control of nanoscale phase transition in vanadium dioxide,” *Light, Sci. Appl.*, vol. 5, no. 10, 2016, Art. no. e16173.
- [6] P. Hosseini, C. D. Wright, and H. Bhaskaran, “An optoelectronic framework enabled by low-dimensional phase-change films,” *Nature*, vol. 511, no. 7508, pp. 206–211, 2014.

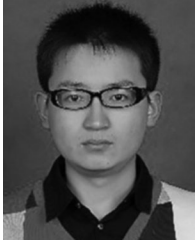
- [7] K.-K. Du *et al.*, "Control over emissivity of zero-static-power thermal emitters based on phase-changing material GST," *Light, Sci. Appl.*, vol. 6, no. 1, 2016, Art. no. e16194.
- [8] T. Tuma, A. Pantazi, M. Le Gallo, A. Sebastian, and E. Eleftheriou, "Stochastic phase-change neurons," *Nature Nanotechnol.*, vol. 11, no. 8, pp. 693–699, 2016.
- [9] D. Lencer, M. Salinga, B. Grabowski, T. Hickel, J. Neugebauer, and M. Wuttig, "A map for phase-change materials," *Nature Mater.*, vol. 7, no. 12, pp. 972–977, 2008.
- [10] N. Yamada, "Origin, secret, and application of the ideal phase-change material GeSbTe," *Phys. Status Solidi B*, vol. 249, no. 10, pp. 1837–1842, 2012.
- [11] N. Yamada, E. Ohno, K. Nishiuchi, N. Akahira, and M. Takao, "Rapid-phase transitions of GeTe-Sb₂Te₃ pseudobinary amorphous thin films for an optical disk memory," *J. Appl. Phys.*, vol. 69, no. 5, pp. 2849–2856, 1991.
- [12] G. W. Burr, B. N. Kurdi, J. C. Scott, C. H. Lam, K. Gopalakrishnan, and R. S. Shenoy, "Overview of candidate device technologies for storage-class memory," *IBM J. Res. Develop.*, vol. 52, pp. 449–464, 2008.
- [13] W. I. Park *et al.*, "Self-assembled incorporation of modulated block copolymer nanostructures in phase-change memory for switching power reduction," *ACS Nano*, vol. 7, pp. 2651–2658, 2013.
- [14] R. E. Simpson *et al.*, "Interfacial phase-change memory," *Nature Nanotechnol.*, vol. 6, no. 8, pp. 501–505, 2011.
- [15] J. Tominaga, A. V. Kolobov, P. Fons, T. Nakano, and S. Murakami, "Ferroelectric order control of the dirac-semimetal phase in GeTe-Sb₂Te₃ superlattices," *Adv. Mater. Interfaces*, vol. 1, no. 1, 2014, Art. no. 1300027.
- [16] J. Tominaga *et al.*, "Giant multiferroic effects in topological GeTe-Sb₂Te₃ superlattices," *Sci. Technol. Adv. Mater.*, vol. 16, no. 1, 2015, Art. no. 014402.
- [17] N.-K. Chen *et al.*, "Origin of high thermal stability of amorphous Ge₁Cu₂Te₃ alloy: A significant Cu-bonding reconfiguration modulated by Te lone-pair electrons for crystallization," *Acta Mater.*, vol. 90, pp. 88–93, 2015.
- [18] J. Hegedus and S. R. Elliott, "Microscopic origin of the fast crystallization ability of Ge-Sb-Te phase-change memory materials," *Nature Mater.*, vol. 7, no. 5, pp. 399–405, 2008.
- [19] X.-B. Li *et al.*, "Role of electronic excitation in the amorphization of Ge-Sb-Te alloys," *Phys. Rev. Lett.*, vol. 107, no. 1, 2011, Art. no. 015501.
- [20] X. P. Wang *et al.*, "Role of the nano amorphous interface in the crystallization of Sb₂Te₃ towards non-volatile phase change memory: Insights from first principles," *Phys. Chem. Chem. Phys.*, vol. 16, no. 22, pp. 10810–10815, 2014.
- [21] N. Takaura *et al.*, "Charge injection super-lattice phase change memory for low power and high density storage device applications," in *Proc. Symp. VLSI Technol.*, Kyoto, Japan, 2013, pp. T130–T131.
- [22] X. Yu and J. Robertson, "Modeling of switching mechanism in GeSbTe chalcogenide superlattices," *Sci. Rep.*, vol. 5, 2015, Art. no. 12612.
- [23] J. Kalikka, X. Zhou, E. Dilcher, S. Wall, J. Li, and R. E. Simpson, "Strain-engineered diffusive atomic switching in two-dimensional crystals," *Nature Commun.*, vol. 7, 2016, Art. no. 11983.
- [24] X. Zhou, J. Kalikka, X. Ji, L. Wu, Z. Song, and R. E. Simpson, "Phase-change memory materials by design: A strain engineering approach," *Adv. Mater.*, vol. 28, no. 15, pp. 3007–3016, 2016.
- [25] T. Ohyanagi and N. Takaura, "Investigation of switching region in superlattice phase change memories," *AIP Adv.*, vol. 6, no. 10, 2016, Art. no. 105104.
- [26] J. Momand *et al.*, "Interface formation of two- and three-dimensionally bonded materials in the case of GeTe-Sb₂Te₃ superlattices," *Nanoscale*, vol. 7, no. 45, pp. 19136–19143, 2015.
- [27] M. C. Lucking, J. Bang, H. Terrones, Y.-Y. Sun, and S. Zhang, "Multivalency-induced band gap opening at MoS₂ edges," *Chem. Mater.*, vol. 27, no. 9, pp. 3326–3331, 2015.
- [28] M. D. Pashley, "Electron counting model and its application to island structures on molecular-beam epitaxy grown GaAs(001) and ZnSe(001)," *Phys. Rev. B*, vol. 40, no. 15, pp. 10481–10487, 1989.
- [29] G. Kresse and J. Furthmüller, "Efficiency of *ab-initio* total energy calculations for metals and semiconductors using a plane-wave basis set," *J. Comput. Mater. Sci.*, vol. 6, pp. 15–50, 1996.
- [30] G. Kresse and J. Furthmüller, "Efficient iterative schemes for *ab initio* total-energy calculations using a plane-wave basis set," *Phys. Rev. B*, vol. 54, 1996, Art. no. 11169.
- [31] G. Kresse and D. Joubert, "From ultrasoft pseudopotentials to the projector augmented-wave method," *Phys. Rev. B*, vol. 59, 1999, Art. no. 1758.
- [32] J. P. Perdew, K. Burke, and M. Ernzerhof, "Generalized gradient approximation made simple," *Phys. Rev. Lett.*, vol. 78, 1996, Art. no. 1396.
- [33] F. London, "The general theory of molecular forces," *Trans. Faraday Soc.*, vol. 33, pp. 8–26, 1937.
- [34] S. Grimme, "Semiempirical GGA-type density functional constructed with a long-range dispersion correction," *J. Comput. Chem.*, vol. 27, no. 15, pp. 1787–1799, 2006.
- [35] X. Wu, M. C. Vargas, S. Nayak, V. Lotrich, and G. Scoles, "Towards extending the applicability of density functional theory to weakly bound systems," *J. Chem. Phys.*, vol. 115, no. 19, pp. 8748–8757, 2001.
- [36] G. Henkelman and H. Jónsson, "Improved tangent estimate in the nudged elastic band method for finding minimum energy paths and saddle points," *J. Chem. Phys.*, vol. 113, no. 22, pp. 9978–9985, 2000.
- [37] G. Henkelman, B. P. Uberuaga, and H. Jónsson, "A climbing image nudged elastic band method for finding saddle points and minimum energy paths," *J. Chem. Phys.*, vol. 113, no. 22, pp. 9901–9904, 2000.
- [38] G. Mills, H. Jónsson, and G. K. Schenter, "Reversible work transition state theory: Application to dissociative adsorption of hydrogen," *Surf. Sci.*, vol. 324, no. 2–3, pp. 305–337, 1995.
- [39] K. Momma and F. Izumi, "VESTA 3 for three-dimensional visualization of crystal, volumetric and morphology data," *J. Appl. Cryst.*, vol. 44, no. 6, pp. 1272–1276, 2011.
- [40] X. Yu and J. Robertson, "Atomic layering, intermixing and switching mechanism in Ge-Sb-Te based chalcogenide superlattices," *Sci. Rep.*, vol. 6, 2016, Art. no. 37325.
- [41] R. Wang, V. Bragaglia, J. E. Boschker, and R. Calarco, "Intermixing during epitaxial growth of van der Waals bonded nominal GeTe/Sb₂Te₃ superlattices," *Cryst. Growth Des.*, vol. 16, no. 7, pp. 3596–3601, 2016.
- [42] B. Casarin *et al.*, "Revisiting the local structure in Ge-Sb-Te based chalcogenide superlattices," *Sci. Rep.*, vol. 6, 2016, Art. no. 22353.
- [43] A. Caretta *et al.*, "Interband characterization and electronic transport control of nanoscaled GeTe/Sb₂Te₃ superlattices," *Phys. Rev. B*, vol. 94, no. 4, 2016, Art. no. 045319.
- [44] M. Hase, P. Fons, K. Mitrofanov, A. V. Kolobov, and J. Tominaga, "Femtosecond structural transformation of phase-change materials far from equilibrium monitored by coherent phonons," *Nat. Commun.*, vol. 6, 2015, Art. no. 8367.
- [45] J. Momand, R. Wang, J. E. Boschker, M. A. Verheijen, R. Calarco, and B. J. Kooi, "Dynamic reconfiguration of van der Waals gaps within GeTe-Sb₂Te₃ based superlattices," *Nanoscale*, vol. 9, no. 25, pp. 8774–8780, 2017.



Nian-Ke Chen received the B.S. and M.S. degrees from Jilin University, Changchun, China, in 2011 and 2014, respectively. He is currently working toward the Ph.D. degree in physical electronics at Jilin University. His research interests include the structures, properties, and phase transitions of phase-change memory materials with first-principles calculations.



Xian-Bin Li received the B.S., M.S., and Ph.D. degrees all in microelectronics from Jilin University, Changchun, China, in 2005, 2007, and 2010, respectively. He is currently an Associate Professor and in-charge of the research Branch of Computational Semiconductor Physics, State Key Laboratory of Integrated Optoelectronics, College of Electronic Science and Engineering, Jilin University. His research interests include the key problems in microelectronics and optoelectronics with the first-principles calculation, including phase-change memory physics, semiconductor defect physics, and 2-D semiconductor design.



Xue-Peng Wang received the B.S. and M.S. degrees from Jilin University, Changchun, China, in 2012 and 2015, respectively. He is currently working toward the Ph.D. degree in physical electronics at Jilin University. His research interests include the structures, properties, and phase transitions of phase-change memory materials with first-principles calculations.



Sheng-Yi Xie received the B.S., M.S., and Ph.D. degrees from Jilin University, Changchun, China, in 2008, 2011, and 2014, respectively. From 2014 to 2016, he was a Postdoctor with the Center for High Pressure Science and Technology Advanced Research. He is currently an Assistant Professor with Hunan University. His research interests include the structures and properties of low-dimensional materials and structure transition under extreme conditions with first-principles calculations.



Wei Quan Tian received the Ph.D. degree from the University of Guelph, Guelph, Canada, in 2001. He was a Postdoctoral Fellow with the University of Ottawa (2001) and with the University of British Columbia (2003) in Canada. In 2004, he was a JSPS Fellow with Kyushu University, in Japan. He was a Full Professor with Jilin University in 2005 and with the Harbin Institute of Technology in 2009, and he also visited the University of Louisville as a Visiting Professor in 2008. He is a Full Professor with Chongqing University. His research interests include nonlinear optical properties simulation up to three photon absorption, structure and properties of alloy clusters, and low-dimensional nanomaterials.



Shengbai Zhang received the Ph.D. degree in physics from the University of California at Berkeley, Berkeley, CA, USA, in 1989. He then joined Xerox PARC, Palo Alto, CA, where he performed postdoctoral research. In 1991, he moved to the National Renewable Energy Laboratory, Golden, CO and became the Group Leader for computational materials science in 2005. In 2008, he was appointed as a Senior Kodosky Constellation Chair with Rensselaer Polytechnic Institute, Troy, NY. He has a broad theoretical research background in computational materials physics, which covers a range of inorganic and organic semiconductors and solids for bulk properties, defect structures, and surface physics. In 2001, he was selected as an APS Fellow.



Hong-Bo Sun received the B.S. and Ph.D. degrees from Jilin University, Changchun, China, in 1992 and 1996, respectively. He was a Postdoctoral Researcher with the University of Tokushima, Japan, from 1996 to 2000, and then an Assistant Professor with the Department of Applied Physics, Osaka University, Japan. In 2005, he was promoted to a Full Professor (Changjiang Scholar) with Jilin University. In September 2017, he moved to Tsinghua University. He has authored or coauthored more than 300 scientific papers, which have been cited more than 12000 times, with an H-factor of 56. His research interests include ultrafast optoelectronics, particularly on laser nanofabrication and ultrafast spectroscopy. In 2017, he was selected as an IEEE Fellow and an OSA Fellow.